ISSN 1063-7834, Physics of the Solid State, 2016, Vol. 58, No. 9, pp. 1782–1791. © Pleiades Publishing, Ltd., 2016.
Original Russian Text © D.A. Balaev, A.A. Krasikov, S.V. Stolyar, R.S. Iskhakov, V.P. Ladygina, R.N. Yaroslavtsev, O.A. Bayukov, A.M. Vorotynov, M.N. Volochaev, A.A. Dubrovskiy, 2016, published in Fizika Tverdogo Tela, 2016, Vol. 58, No. 9, pp. 1724–1732.

MAGNETISM

Change in the Magnetic Properties of Nanoferrihydrite with an Increase in the Volume of Nanoparticles during Low-Temperature Annealing

D. A. Balaev[a, b, *], A. A. Krasikov[a, b], S. V. Stolyar[a, b], R. S. Iskhakov[a], V. P. Ladygina[c], R. N. Yaroslavtsev[b], O. A. Bayukov[a], A. M. Vorotynov[a], M. N. Volochaev[a], and A. A. Dubrovskiy[a, d]

[a] *Kirensky Institute of Physics, Siberian Branch of the Russian Academy of Sciences, Akademgorodok 50/38, Krasnoyarsk, 660036 Russia*

[b] *Siberian Federal University, Svobodny pr. 79, Krasnoyarsk, 660041 Russia*

[c] *International Scientific Centre for Organism Extreme States Research, Presidium of the Krasnoyarsk Scientific Centre of the Siberian Branch of the Russian Academy of Sciences, Akademgorodok 50, Krasnoyarsk, 660036 Russia*

[d] *International Laboratory of High Magnetic Fields and Low Temperatures, ul. Gajowicka 95, Wroclaw, 53-421 Poland*

** e-mail: dabalaev@iph.krasn.ru*

Received February 11, 2016

Abstract—The results of the investigation into the effect of low-temperature annealing of a powder of nanoparticles of bacterial ferrihydrite on its magnetic properties have been presented. It has been found that an increase in the time (up to 240 h) and temperature (in the range from 150 to 200°C) of annealing leads to a monotonic increase in the superparamagnetic blocking temperature, the coercive force, and the threshold field of the opening of the magnetic hysteresis loop (at liquid-helium temperatures), as well as to an increase in the magnetic resonance line width at low temperatures and in the magnetic susceptibility at room temperature. At the same time, according to the results of the analysis of the Mössbauer spectra, the annealing of ferrihydrite does not lead to the formation of new iron oxide phases. Most of these features are well consistent with the fact that the low-temperature annealing of ferrihydrite causes an increase in the size of nanoparticles, which is confirmed by the results of transmission electron microscopy studies.

DOI: 10.1134/S1063783416090092

1. INTRODUCTION

Ferrihydrite is a metastable material, which is widespread in aquatic systems and exists in the nanoscale form. The chemical formula of ferrihydrite is usually written in the following form: $5Fe_2O_3 \cdot 9H_2O$. However, the presence of defects in the structure can lead to a change in both the number of OH bonds and the content of "water." The magnetic moments of iron atoms in the ferrihydrite structure are ordered antiferromagnetically. At the same time, owing to a number of factors, such as the presence of defects and a large surface area of the particles in the structure, ferrihydrite nanoparticles acquire an uncompensated magnetic moment [1, 2]. This has opened up new possibilities for practical applications of ferrihydrite nanoparticles, for example, for the targeted drug delivery in the human body [3, 4].

The magnetic properties of an ensemble of nanoparticles of ferrihydrite (including its "biogenic analogue"—ferritin) exhibit interesting features: the superparamagnetic (SP) behavior, the characteristic blocking temperature T_B, the magnetization hysteresis curve $M(H)$ at temperatures in the range $T < T_B$, and the shift of the magnetic hysteresis loop upon cooling in an external magnetic field from a temperature higher than the blocking temperature, as well as the nontrivial temperature evolution of the uncompensated magnetic moment and the antiferromagnetic (AF) susceptibility [5–19]. It is obvious that, in order to determine the mechanisms responsible for the magnetic properties of ferrihydrite nanoparticles, it is advisable to compare the results obtained for ferrihydrite particles of different sizes. In addition, it should be noted that the purposeful modification of the sizes of magnetic nanoparticles is important for practical applications, because the effective drug delivery requires the use of an optimal ratio between the magnetic moment of the particles (in fact, the magnetic susceptibility) and their linear sizes.

Preliminary investigations [20] showed that low-temperature annealing (at 150°C) of biogenic ferrihydrite (in a powder form) leads to a substantial increase in the blocking temperature. Moreover, the analysis of the magnetization curves of the initial sample and the sample subjected to annealing for 3 h revealed an increase in the magnetic momentum of the ferrihydrite particles, which indicates an increase in their sizes [19].

Nanoparticles of the biogenic ferrihydrite are formed as a result of the vital activity of bacteria [21–23]. This paper presents detailed results of the investigation of the influence exerted by the temperature (in the range of 150–200°C) and low-temperature annealing time on the magnetic properties of the nanoparticles of this material. One of the objectives of this study was to reveal the technique that would make it possible to control the increase in the size of ferrihydrite nanoparticles during the low-temperature annealing.

2. SAMPLE PREPARATION AND EXPERIMENTAL TECHNIQUE

The method used in this study for the sample preparation is based on the cultivation of microorganisms (bacteria *Klebsiella oxytoca*) under anaerobic conditions [21–23]. Ferrihydrite is formed as a by-product of the vital activity of bacteria. The ferrihydrite bacterial residues were subjected to repeated ultrasonic treatment followed by their washing and centrifuging with the formation of a stable sol of nanoparticles in an aqueous solution, which was subsequently dried. For samples of different batches prepared by this method, the spread of the superparamagnetic blocking temperature (in an external magnetic field $H = 1$ kOe) did not exceed three degrees. In the preparation of this series of samples, the gadolinium salt was added to the culture medium. The X-ray fluorescence analysis demonstrated that the content of rare-earth elements in the samples was within the error.

The initial powder of magnetic nanoparticles prepared by the new synthesis (hereinafter, designated as sample 0 h) was subjected to low-temperature annealing in an air atmosphere for different periods of time (up to 10 days) at temperatures of 150 and 200°C. The annealed samples were designated in accordance with their annealing time and temperature, for example, sample 240 h (200°C). It was found that, upon annealing, the weight of the initial powder of ferrihydrite nanoparticles decreased by approximately 15–20%. In the authors' opinion, this is explained by the loss of intergranular "water" (OH groups) and by the partial sublimation of the organic layer on the surface of nanoparticles.

The electron microscopic examination was carried out at the Center for Collective Use of the Krasnoyarsk Scientific Center of the Siberian Branch of the Russian Academy of Sciences (Krasnoyarsk, Russia) on a Hitachi HT7700 transmission electron microscope operating at an accelerating voltage of 100 kV. The samples were prepared by stirring a powder of nanoparticles in an alcoholic solution in an ultrasonic bath, followed by applying the prepared suspension to supporting grids with a perforated carbon coating.

The Mössbauer spectra were measured on an MS-1104Em Mössbauer spectrometer with a ^{57}Co(Cr) source at room temperature for powder samples with a thickness of 5–10 mg/cm^2 according to the natural iron content. The isomer chemical shifts are given relative to the α-Fe.

The magnetic measurements were performed on a vibrating-sample magnetometer [24]. The powder under investigation was fixed in a measuring cell filled with paraffin. The data on the magnetic moment are presented below in units of emu per unit mass of the studied powder. The temperature dependences of the magnetic moment $M(T)$ were measured in the modes of cooling without a magnetic field (zero field cooling (ZFC)) and cooling in an external magnetic field (field cooling (FC)).

The magnetic resonance spectra were recorded on a Bruker ELEXSYS 560 spectrometer operating in the X range at the characteristic frequency of microwave radiation of ~9.4 GHz in the temperature range from 100 to 300 K.

3. RESULTS

3.1. Results of the Mössbauer Spectroscopy and Transmission Electron Microscopy

The results of transmission electron microscopy studies of the initial sample and the sample subjected to a 24-hour annealing at a temperature of 200°C are presented in Fig. 1. It can be seen from this figure that the size of nanoparticles in the annealed sample is slightly larger than that in the initial sample. The average size of nanoparticles (according to the data obtained from several micrographs) was found to be equal to ~2.7 nm for the initial sample, which is in agreement with the previously obtained data [25], and ~4 nm for the annealed sample. The increase in the size of nanoparticles in the sample after the low-temperature annealing is consistent with the results of our previous studies [19, 20], in which this conclusion was drawn based on the analysis of the magnetization curves and the increase in the blocking temperature.

The X-ray diffraction patterns of the powders prepared by the method described above are characteristic of the amorphous state [26]. Therefore, in order to identify the crystal-chemical structure and to obtain information about possible changes in the local environment of iron atoms, as well as about the formation of other iron oxide phases during the annealing, we

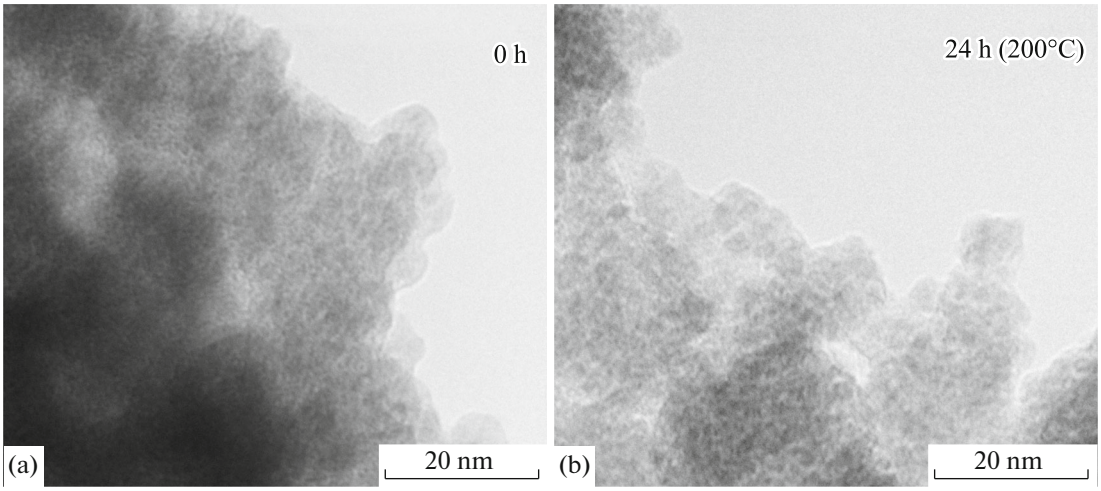

Fig. 1. Transmission electron microscopy images of the samples annealed for (a) 0 h and (b) 24 h (200°C).

used the Mössbauer spectroscopy. The Mössbauer spectra measured at room temperature for the initial sample and the sample annealed for 240 h at 150°C are shown in Fig. 2a. The spectra have the form of quadrupole doublets, which are characteristic of unblocked superparamagnetic nanoparticles, with different degrees of line broadening. The analysis of the distribution of the quadrupole splittings P(QS) in the experimental spectra (Fig. 2b) leads to the conclusion that there are at least three nonequivalent positions of iron with different degrees of distortion of the local environment. The model spectra (lines in Fig. 2a) were formed taking into account the specific features observed in the distribution P(QS) and then were fitted to the experimental spectra by varying the entire set of hyperfine parameters. The results of the interpretation of the Mössbauer spectra are summarized in Table 1. The iron positions designated as Fe1 and Fe2 (in accordance with the results of previous studies [22, 26]) correspond to the cubic and hexagonal packings of the ligands, respectively, whereas the Fe3 positions correspond to interlayer iron atoms. The parameters of the model spectra are in good agreement with the previously obtained results for ferrihydrite [22, 26]. Moreover, the annealing does not lead to the appearance of specific features that would indicate the formation of new phases of hydroxide or iron oxide.

3.2. Temperature Dependences of the Magnetic Moment. An Increase in the Blocking Temperature during Annealing

Figure 3 illustrates the influence of the annealing time at different temperatures, i.e., 150°C (Fig. 3a) and 200°C (Fig. 3b), on the temperature dependences of the magnetic moment $M(T)$ of the ferrihydrite nanoparticles. These dependences are characterized by two temperatures, namely, the temperature T_{irr}, which corresponds to the irreversible behavior of the magnetic moment in the FC and ZFC modes, and the temperature T_{max}, which corresponds to the maximum in the dependence $M(T)$. Examples of the determination of the temperatures T_{irr} and T_{max} are shown in Fig. 3b. It can be seen from Fig. 3 that, as the annealing time increases, the two characteristic temperatures increase, and at a higher annealing temperature, this effect is more pronounced.

Table 1. Mössbauer parameters of bacterial ferrihydrite (IS is the isomer shift, QS is the quadrupole splitting, W is the line width, and A is the occupancy of the iron positions. The iron positions designated as Fe1 and Fe2 correspond to the cubic and hexagonal packings of the ligands, respectively, and the Fe3 positions correspond to the interlayer iron atoms)

Sample	IS (±0.005 mm/s)	QS (±0.01 mm/s)	W (±0.01 mm/s)	A (±0.03)	Position
0 h	0.348	0.532	0.356	0.521	Fe1
	0.349	0.868	0.310	0.320	Fe2
	0.347	1.212	0.328	0.159	Fe3
240 h (150°C)	0.339	0.575	0.373	0.541	Fe1
	0.342	0.934	0.326	0.334	Fe2
	0.345	1.323	0.324	0.125	Fe3

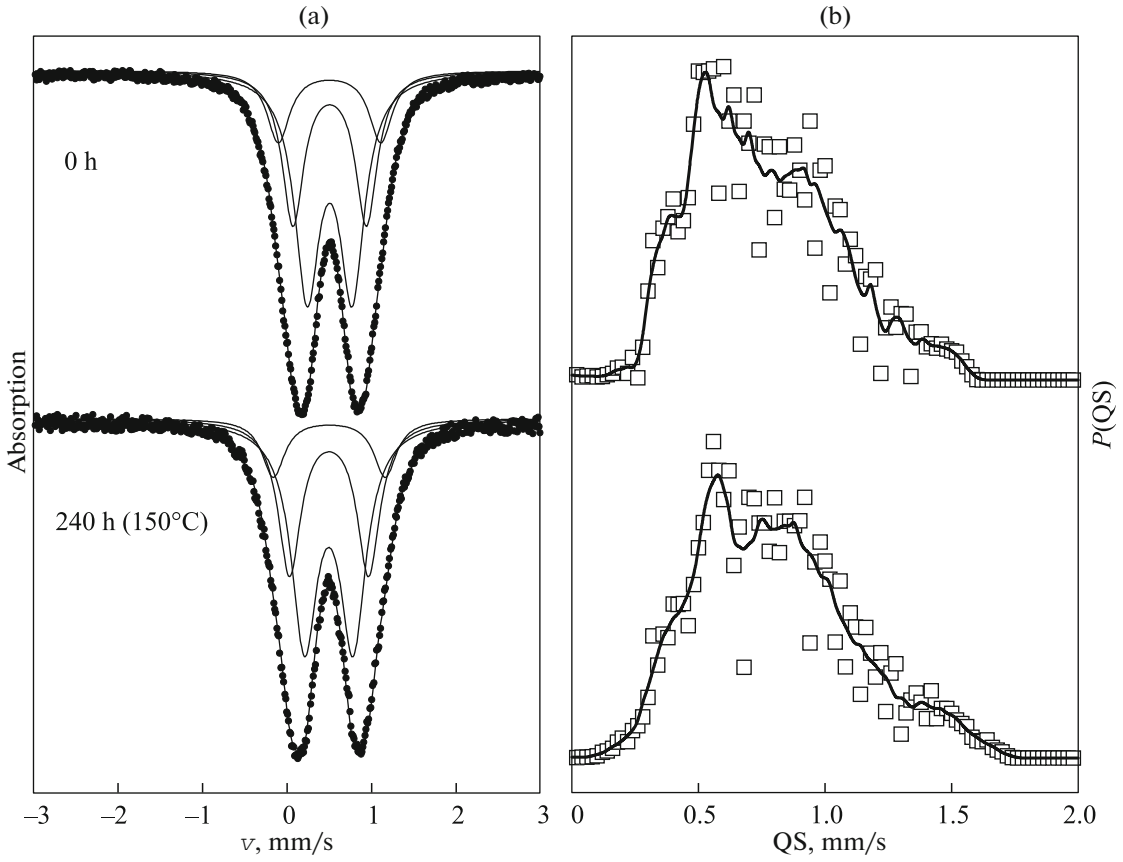

Fig. 2. (a) Mössbauer spectra at room temperature and (b) distribution of the quadrupole splitting P(QS) of the samples annealed for 0 h and 240 h (150°C). The solid lines show the partial doublets forming the total spectrum.

Usually, the value of T_{irr} for an ensemble of superparamagnetic nanoparticles is slightly higher than the value of T_{max}, because the temperature T_{irr} corresponds to the blocking temperature of the largest-size particles and the relationship between the temperatures T_{max} and T_{irr} depends on the particle size distribution [27]. However, as can be seen from the data presented in Fig. 3, the annealed samples in most cases satisfy the relationship $T_{irr} < T_{max}$. A similar behavior of the dependences $M(T)$ was also observed by other authors for samples of synthetic ferrihydrite nanoparticles [6, 8]. At the same time, as the external magnetic field increases, the behavior of the dependences $M(T)$ becomes typical of superparamagnetic systems. This is illustrated in Fig. 4, which shows the dependences $M(T)/H$ for the sample subjected to annealing for 24 h at 220°C in different external magnetic fields. It can be seen from this figure that, with an increase in the external magnetic field, both characteristic temperatures (T_{irr} and T_{max}) decrease, and in the magnetic fields H = 5 and 10 kOe, the dependences exhibit a typical behavior: $T_{irr} > T_{max}$.

An approximate form of the particle size distribution over the blocking temperatures can be determined by analyzing the behavior of the dependence $d(M(T)_{ZFC}-M(T)_{FC})/dT$ [27, 28]. The maximum of this dependence can be considered to be the average blocking temperature $\langle T_B\rangle$[1] of the particles [27, 28]. The dependences $d(M(T)_{ZFC}-M(T)_{FC})/dT$ obtained for selected samples from the data presented in Fig. 3 are shown in Fig. 5. As can be seen from Fig. 5, the annealing substantially changes the distribution function: an increase in the annealing time leads to an increase in the average blocking temperature $\langle T_B\rangle$, the range of the particle size distribution over the blocking temperatures becomes wider (the value of T_{irr} increases), and the observed change is more pronounced in the case of a higher annealing temperature. The obtained information about the influence of the annealing on the characteristic temperatures $\langle T_B\rangle$, T_{irr}, and T_{max} is summarized in Table 2.

The blocking temperature for noninteracting superparamagnetic particles is uniquely related to the particle volume V in accordance with the Néel–Brown expression

$$T_B = KV/\ln(\tau/\tau_0)k. \quad (1)$$

[1] For the log-normal distribution, the average blocking temperature $\langle T_B\rangle$ corresponds to the average size of the particles [28].

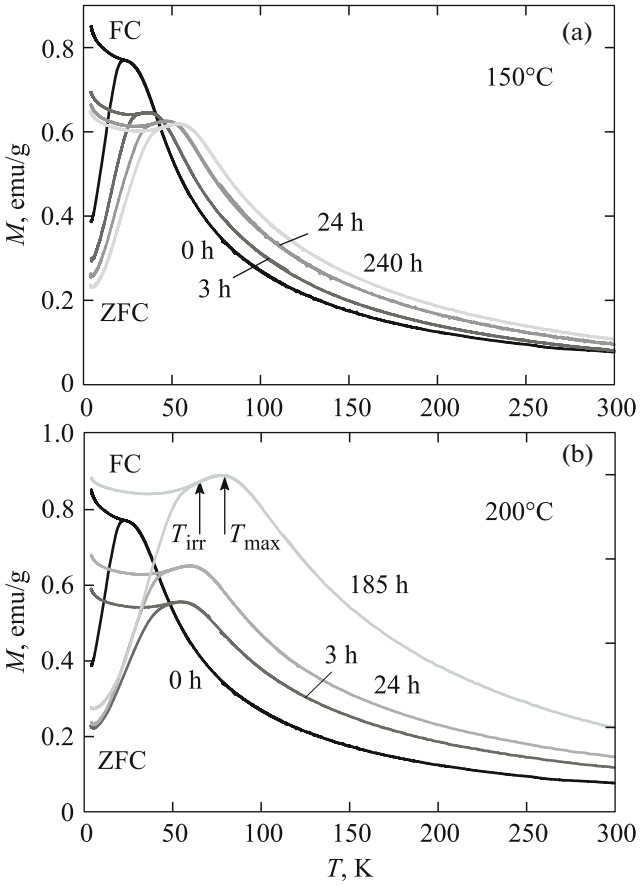

Fig. 3. Temperature dependences of the magnetic moment $M(T)$ measured under the conditions ZFC and FC (H = 1 kOe) for the initial sample and samples after annealing at temperatures of (a) 150 and (b) 200°C. Panel (b) shows examples of the determination of the temperatures T_{max} and T_{irr}.

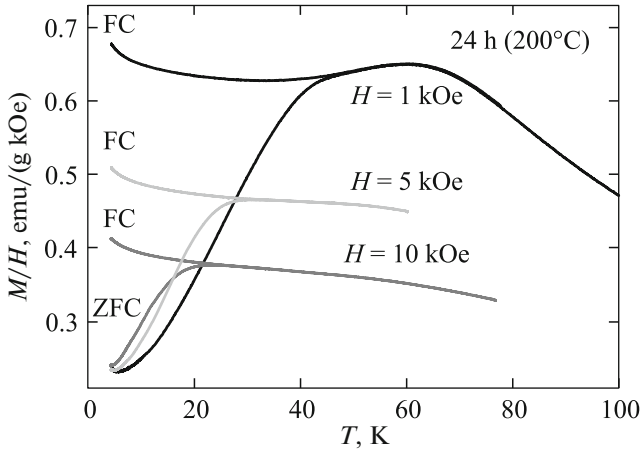

Fig. 4. Temperature dependences $M(T)/H$ of the sample annealed for 24 h (200°C) under the conditions ZFC and FC in different external magnetic fields H.

Here, K is the constant of magnetic anisotropy, k is the Boltzmann constant, τ is the characteristic time of observation (measurement), and τ_0 is the superparamagnetic relaxation time of the particle. The measurement time τ depends on the method of investigation. For example, for static magnetic measurements, the measurement time is $\tau \sim 10^1$–10^2 s, whereas for Mössbauer spectroscopy, it is equal to $\sim 5 \times 10^{-9}$ s [1]. Using the values of $\tau_0 \sim 10^{-11}$ s for ferrihydrite nanoparticles [9, 10], from expression (1), we find that the blocking temperature obtained for the Mössbauer technique should be approximately five times higher than the blocking temperature observed in static magnetic measurements. This agrees well with the fact that the values of $\langle T_B \rangle$ for the studied samples do not exceed 35 K (see Table 2), while the Mössbauer spectra at room temperature are characteristic of the unblocked state of the nanoparticles.

According to the results obtained from the analysis of the Mössbauer spectra, upon annealing of ferrihydrite, neither the formation of new iron oxide phases nor a significant change in the crystal-chemical structure of the nanoparticle occur. Therefore, based on relationship (1), the increase in the temperatures $\langle T_B \rangle$, T_{irr}, and T_{max} after the annealing can be reasonably related to the increase in the size of nanoparticles. This is confirmed by the results of transmission electron microscopy studies (Fig. 1). It should be noted that changes in the values of the characteristic temperatures $\langle T_B \rangle$ and T_{irr} with an increase in the annealing time and temperature provide a more accurate information about the increase in the linear sizes d of nanoparticles as compared to the results of transmission electron microscopic studies, because $T_B \sim V$ and $d \sim V^{1/3} \sim T_B^{1/3}$. The relative increase in the average size of nanoparticles in the annealed samples is reflected in Table 2 (column 5).

It is reasonable to assume that an increase in the nanoparticle size during the low-temperature annealing is caused by their agglomeration. Indeed, if the formation of nanoparticles occurs at room temperature (see Section 2), then, at temperatures of annealing, there is a partial loss of intergranular "water," and the sublimation of the organic shell results in the agglomeration of closely spaced nanoparticles. These processes are strongly influenced by the annealing time and temperature (the annealing at higher temperatures of ~300°C already leads to a change in the phase composition of the nanoparticle [26]).

3.3. Magnetic Hysteresis

The magnetic hysteresis loops at $T = 4.2$ K for the unannealed sample (sample 0 h) and the samples subjected to annealing for 24 h are shown in Fig. 6. It can be seen from this figure that, in the maximum applied magnetic field $H_{max} = 60$ kOe, the magnetic hysteresis loops at $T = 4.2$ K are open. Nevertheless, it can be

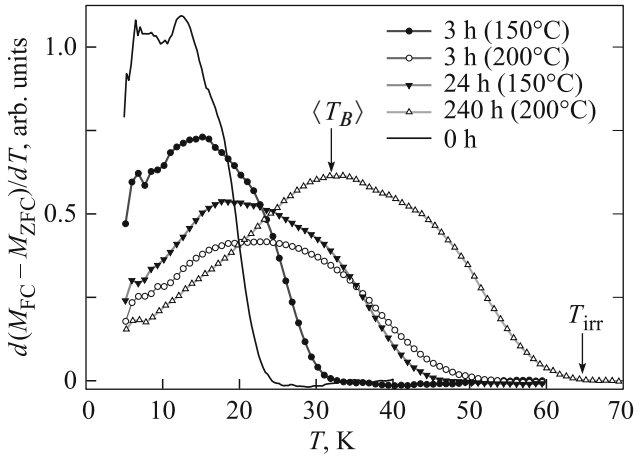

Fig. 5. Temperature dependences $d(M(T)_{ZFC}-M(T)_{FC})/dT$ obtained for selected samples from the data presented in Fig. 3. Examples of the determination of the temperatures $\langle T_B\rangle$ and T_{irr} are shown.

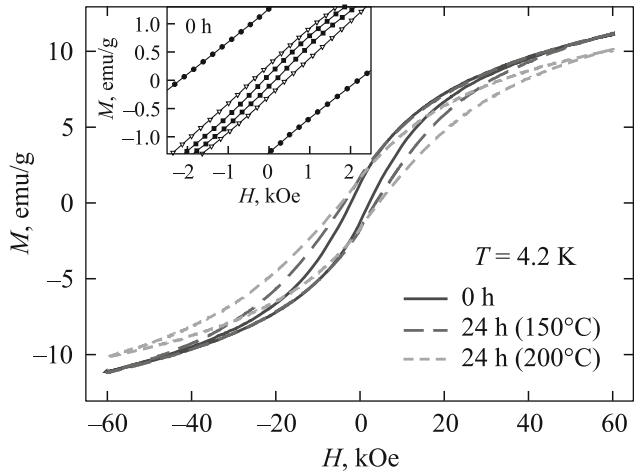

Fig. 6. Hysteresis dependences $M(H)$ at $T = 4.2$ K for the samples annealed for 0 h, 24 h at 150°C, and 24 h at 200°C. The inset shows parts of the dependences $M(H)$ near the origin of the coordinates for the unannealed sample (sample 0 h) at temperatures of 4.2 (circles), 13 (triangles), and 18 K (squares).

stated that the coercive force H_C in the magnetic field $H_{max} = 60$ kOe increases for the annealed samples. The inset in Fig. 6 shows parts of the magnetic hysteresis loops measured for the unannealed sample (0 h) at temperatures of 4.2, 13, and 18 K (for $T = 13$ and 18 K, the hysteresis dependences $M(H)$ at $H_{max} = 60$ kOe are already limiting).

For magnetic nanoparticles, the coercive force H_C is determined by the expression following from the Stoner–Wohlfarth model [29]:

$$H_C = K/M_S\{1 - (T/T_B^{0.5}\}, \quad (2)$$

Table 2. Characteristic temperatures T_{max}, T_{irr}, and $\langle T_B\rangle$ (examples of their determination are shown in Figs. 3 and 5), the coercive force H_C at $T = 4.2$ K and $H_{max} = 60$ kOe, and the parameter $(\langle T_B\rangle/12.5\text{ K})^{1/3}$, which characterizes the relative increase in the average size of nanoparticles in the samples

Sample	T_{max}, K	T_{irr}, K	$\langle T_B\rangle$, K	$(\langle T_B\rangle/12.5\text{ K})^{1/3}$	H_C, kOe
0 h	23.3	22.8	12.5	1	2.2
3 h (150°C)	35.5	32	14.7	1.06	3.2
8 h (150°C)	47	39	16.0	1.07	3.9
24 h (150°C)	47.5	38.5	17.0	1.09	3.8
74 h (150°C)	51	42.5	17.2	1.11	4.05
240 h (150°C)	53.5	44	18.0	1.13	4.2
3 h (200°C)	55	50	22.5	1.21	4.4
8 h (200°C)	59	47	23.6	1.24	4.4
24 h (200°C)	60	48	24.4	1.25	4.45
72 h (200°C)	69	61	29.5	1.33	4.6
185 h (200°C)	77.5	65	32.5	1.38	4.7

where M_S is the saturation magnetization. According to our data, the coercive force H_C in the magnetic field $H_{max} = 60$ kOe varies with temperature much more rapidly than the dependence of $\{1 - (T/T_B)^{0.5}\}$. This can be caused by the influence of the particle size distribution over the blocking temperatures [30]. Nevertheless, if we restrict ourselves to the data at $T = 4.2$ K, then, from expression (2), we can obtain the dependence of the coercive force H_C on the particle size by taking into account that $M_S = \mu_P/V$. The magnetic moment of the antiferromagnetic particle μ_P depends on its volume as follows: $\mu_P \sim V^n$, where the exponent n is determined by the type of defects [31]. According to the results of numerous studies of ferrihydrite and ferritin [1, 5, 6, 8, 11–14, 18, 19], it is established that, for these materials, $\mu_P \sim V^{1/2}$. Therefore, we have $M_S \sim V^{-1/2}$ and $H_C = KV^{1/2}\{1 - (T/T_B)^{0.5}\}$. The obtained expression explains the increase in the coercive force H_C at $T = 4.2$ K and $H_{max} = 60$ kOe for the annealed samples. Moreover, in this case, there is a good correlation between the coercive force $H_C(H_{max} = 60$ kOe, $T = 4.2$ K) and the temperatures T_{max} and $\langle T_B\rangle$ (see Table 2). Thus, despite the fact that the magnetic hysteresis loops $M(H)$ at $T = 4.2$ K remain open in the magnetic field $H_{max} = 60$ kOe, the coercive force $H_C(H_{max} = 60$ kOe, $T = 4.2$ K) can serve as a characteristic of the increase in the nanoparticle size. This is further confirmed by the relatively weak dependence $H_C(H_{max})$ in the range of magnetic fields above 50 kOe (see Fig. 7a).

In addition to the increase in the coercive force H_C, we revealed another difference in the behavior of partial magnetic hysteresis loops of the annealed samples.

Figure 7 illustrates the dependences of the coercive force H_C (Fig. 7a) and the residual magnetic moment M_R (Fig. 7b) on the maximum applied magnetic field H_{max} for the samples annealed for 0 h and 24 h (200°C). In these experiments, the magnetic hysteresis loops were measured to different absolute values $|H_{max}|$ with a gradual increase in H_{max}. The insets to Fig. 7 illustrate parts of these loops in the vicinity of the origin of the coordinates (shown in the figure are the partial magnetic hysteresis loops measured to $|H_{max}| = 45$ kOe). Noteworthy is the behavior of the partial magnetic hysteresis loops in the range of weak magnetic fields, where either the loops are still not opened (sample 24 h (200°C) in the inset to Fig. 7a) or the values of H_C and M_R change slightly (sample 0 h in the inset to Fig. 7b). This specific feature is associated with the fact that, in order to overcome the potential barrier caused by the magnetic anisotropy KV, the magnetic moment requires the energy $\mu_P H$, which exceeds the value of this barrier. If the Zeeman energy is less than the energy of the magnetic anisotropy, then, as the external magnetic field decreases to zero, the values of M_R and H_C become equal to zero. In the unannealed sample (sample 0 h), apparently, there are particles characterized by a low value of the magnetic anisotropy KV, as well as by a slight increase in the values of $H_C(H_{max})$ and $M_R(H_{max})$ to a threshold field $H^* \approx 7$ kOe. For $H > H^*$, the dependences $H_C(H_{max})$ and $M_R(H_{max})$ increase more rapidly. For the sample annealed for 24 h at 200°C, the threshold field is significantly higher (≈10 kOe), which is naturally explained by larger sizes of the nanoparticles. In fact, since the magnetic moment satisfies the relationship $\mu_P \sim V^{1/2}$, the Zeeman energy, to a first approximation, is proportional to $V^{1/2}$, whereas the magnetic anisotropy energy is proportional to V; i.e., with an increase in the nanoparticle size, it increases more rapidly.

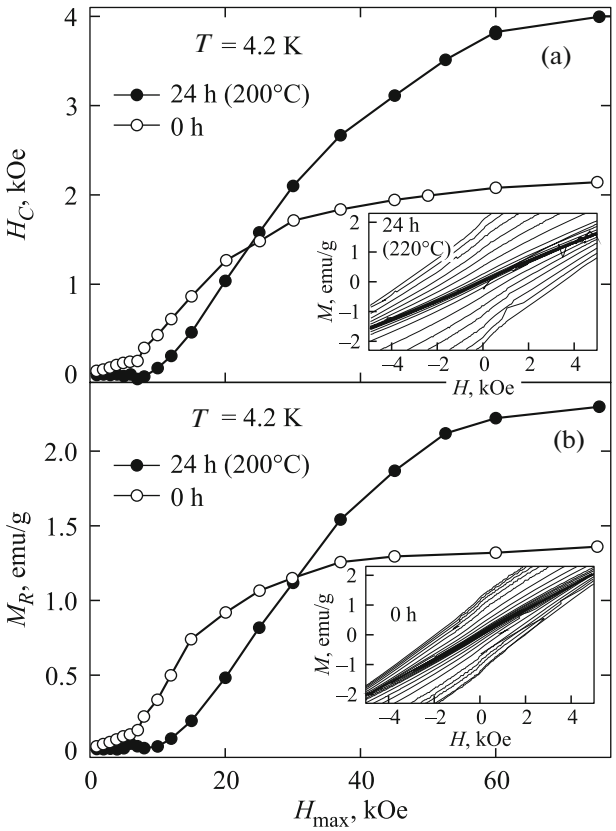

Fig. 7. Dependences of (a) the coercive force H_C and (b) the residual magnetic moment M_R of the samples annealed for 0 h and 24 h (200°C) on the maximum magnetic field H_{max}. The insets in panels (a) and (b) illustrate the partial magnetic hysteresis loops of the samples annealed for 24 h (200°C) and 0 h near the origin of the coordinates in different magnetic fields H_{max}.

3.4. Magnetic Resonance

The magnetic resonance spectra measured for samples 0 h and 240 h (150°C) at different temperatures are shown in Figs. 8a and 8b, respectively. The spectra have the form of single Lorentzian lines with the following parameters at room temperature: $\Delta H \sim$ 1000 Oe with the factors $g = 2.01$ (sample 0 h) and 2.03 (sample of 240 h (150°C)). The resonance fields for both samples slightly decrease with decreasing temperature. The weak dependence of the resonance field on the temperature is characteristic of an ensemble of noninteracting (or weakly interacting) magnetic nanoparticles. The Lorentzian shape of the magnetic resonance signal line for all the studied temperatures suggests either a weak influence of the demagnetizing factors of nanoparticles or their almost spherical shape.

The temperature behavior of the magnetic resonance line widths for samples 0 h and 240 h (150°C) is illustrated in Fig. 8c. It can be seen from this figure that the line width increases monotonically with a decrease in the temperature for both samples and reaches a plateau (saturation) at room temperature. Such a behavior, in our opinion, is caused by an increase of local fields in the samples with a decrease in the temperature. This conclusion is confirmed by the fact that the line width for the sample annealed for 240 h at 150°C increases much more rapidly than that for the unannealed sample (sample 0 h). Indeed, according to the data of static magnetic measurements, the magnetization of the sample annealed for 240 h at 150°C exceeds the magnetization of the unannealed sample (0 h) by more than two times at a temperature of 100 K. At room temperature, this difference is significantly less pronounced. In turn, an increase in the magnetization of the samples is directly related to the sizes of nanoparticles therein (see Table 2 and Fig. 3).

Thus, the temperature behavior of line width confirms the conclusion that the size of nanoparticles in the sample annealed for 240 h at 150°C is larger than

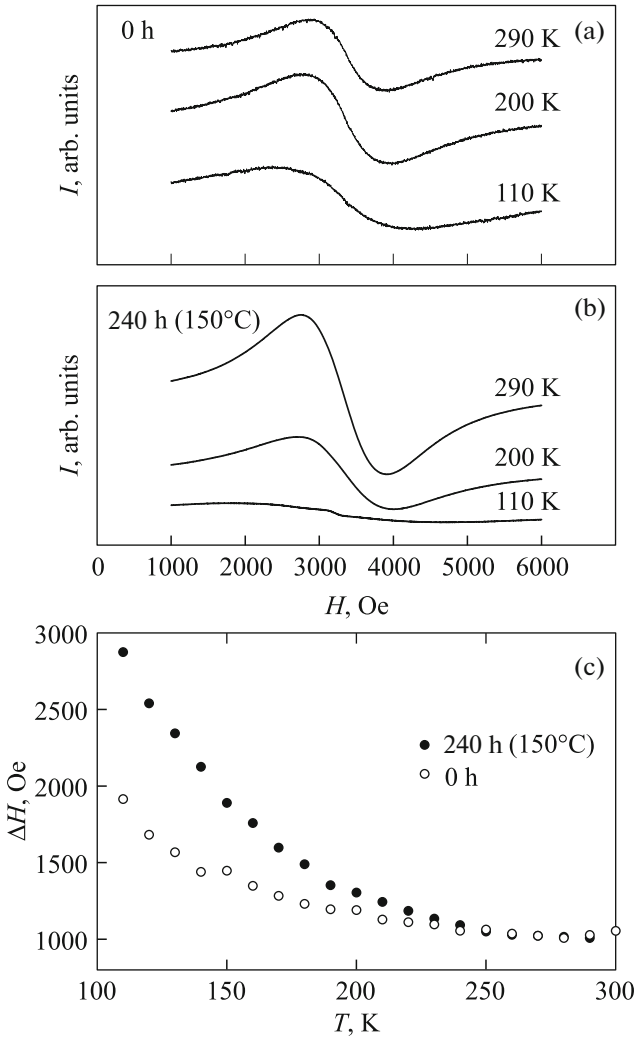

Fig. 8. Magnetic resonance spectra measured for samples (a) 0 h and (b) 240 h (150°C) at the temperatures indicated near the curves. (c) Temperature dependence of the absorption line width ΔH for these samples.

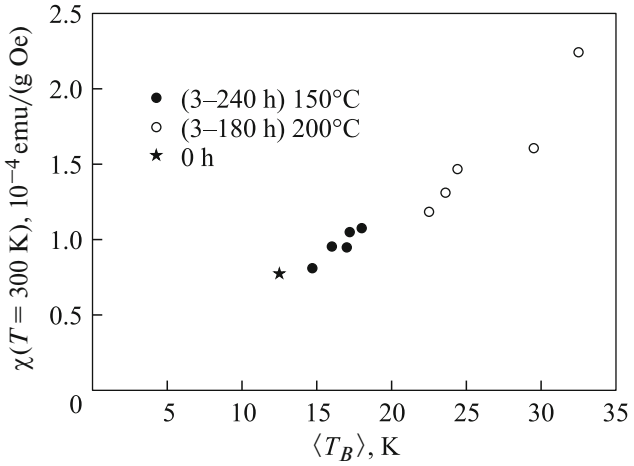

Fig. 9. Dependence of the magnetic susceptibility χ(300 K) on the average blocking temperature $\langle T_B \rangle$ for the studied series of samples.

that in the unannealed sample (sample 0 h). A similar comparison of the line widths of the magnetic resonance signals detected at low temperatures can be used as an indirect method for obtaining information about the relative size of nanoparticles in different samples.

3.5. Magnetic Susceptibility in the Unblocked State

The magnetic susceptibility of an ensemble of antiferromagnetic nanoparticles in the unblocked state ($T > T_B$) is determined by the superparamagnetic response of the system χ_{SP} and the antiferromagnetic susceptibility of the antiferromagnet χ_{AF} [1]: $\chi = \chi_{SP} + \chi_{AF}$. In turn, the superparamagnetic response of the system is determined by the expansion of the Langevin function into a series (which is valid in weak magnetic fields) and can be written as $\chi_{SP} \sim N\langle\mu_P\rangle^2/3kT$, where N is the number of nanoparticles per unit mass (or per unit volume) and $\langle\mu_P\rangle$ is the average magnetic moment per nanoparticle. The number of nanoparticles N is inversely proportional to the nanoparticle volume ($N \sim 1/V$) and, as was noted above, the magnetic moment satisfies the relationship $\mu_P \sim V^{1/2}$. As a result, we find that the superparamagnetic contribution to the magnetic susceptibility does not depend on the nanoparticle size [32], i.e., χ_{SP} = const.[2] Figure 9 shows the dependence of χ(300 K) = M(300 K)/H on the average blocking temperature $\langle T_B \rangle$ (Fig. 5, Table 2) for the series of samples under investigation. For the majority of the samples, the linear dependence of χ(300) on the average blocking temperature $\langle T_B \rangle$ or, in fact, on the average nanoparticle volume V holds with a high accuracy. This fact can be nontrivial, because, if χ_{SP} = const, then an increase in the nanoparticle size leads to a significant increase in the antiferromagnetic susceptibility χ_{AF}(300 K). The inclusion of the mass loss of the sample (no more than 20% during the longest annealing, see Section 2) in the analysis does not fundamentally affect the character of the dependence of the magnetic susceptibility χ(300 K) on the average blocking temperature $\langle T_B \rangle$. From the analysis of the magnetization curves for ferrihydrite and ferritin, it is known that the antiferromagnetic susceptibility χ_{AF} decreases with an increase in the temperature [5–7, 13–15]. This fact still remains unexplained, as well as the sufficiently large values of χ_{AF} for ferrihydrite and ferritin. It is possible that the temperature evolution of the antiferromagnetic susceptibility χ_{AF} differs for different sizes of particles. The revealed linear character of the dependence of the magnetic susceptibility

[2] For NiO nanoparticles with the magnetic moment $\mu_P \sim V^{1/3}$, the superparamagnetic contribution to the magnetic susceptibility is estimated as $\chi_{SP} \sim V^{-1/3} \sim 1/d$, which was observed in [32].

χ(300 K) on the blocking temperature requires further analysis. Nevertheless, the magnetic susceptibility of a powder of ferrihydrite nanoparticles at room temperature can be used to indirectly control the increase in their size upon low-temperature annealing.

4. CONCLUDING REMARKS

Thus, in this work, we investigated the magnetic properties of an ensemble of nanoparticles of biogenic ferrihydrite after the low-temperature annealing (at 150 and 200°C) for different times (up to 10 days). The analysis of the obtained results allowed us to conclude that the annealing leads to an increase in the size of nanoparticles. This conclusion is confirmed by the results of transmission electron microscopy studies. The increase in the size of nanoparticles is associated with their agglomeration. Moreover, the average size of the ferrihydrite nanoparticles can be "controlled" by increasing the temperature (at least to 200°C) and time of the annealing. An increase in the volume of nanoparticles leads to a monotonic increase in the superparamagnetic blocking temperature, the numerical value of the coercive force (at 4.2 K), the characteristic threshold field of the opening of the magnetic hysteresis loop, and the magnetic resonance line width (at low temperatures). Furthermore, it was found that the magnetic susceptibility at room temperature (in the unblocked state) increases approximately linearly with an increase in the blocking temperature (which is proportional to the average volume of the nanoparticles). Although the mechanisms responsible for this type of dependence of the magnetic susceptibility $\chi(T = 300\ \text{K})$ on the blocking temperature T_B have not yet been revealed, the observed dependence makes it possible to perform rapid control of the increase in the size of ferrihydrite nanoparticles during the low-temperature annealing by a rather simple method (measurement of the magnetic susceptibility). The possibility of a targeted and controlled increase in the magnetic susceptibility of ferrihydrite nanoparticles, which was demonstrated in this study, opens the way to determine optimal sizes of nanoparticles for medical applications [4].

ACKNOWLEDGMENTS

We would like to thank S.V. Komogortsev for his participation in the discussion of the results obtained in this work.

This study was supported by the Ministry of Education and Science of the Russian Federation within the State Task for 2014–2016.

REFERENCES

1. S. Mørup, D. E. Madsen, C. Fradsen, C. R. H. Bahl, and M. F. Hansen, J. Phys.: Condens. Matter. **19**, 213202 (2007).
2. Yu. L. Raikher and V. I. Stepanov, J. Exp. Theor. Phys. **107** (3), 435 (2008).
3. Q. A. Pankhurst, N. T. K. Thanh, S. K. Jones, and J. Dobson, J. Phys. D: Appl. Phys. **42**, 224001 (2009).
4. K. Dobretsov, S. Stolyar, and A. Lopatin, Acta Otorhinolaryngol. Ital. **35** (2), 97 (2015).
5. S. A. Makhlouf, F. T. Parker, and A. E. Berkowitz, Phys. Rev. B: Condens. Matter **55** (22), R14717 (1997).
6. M. S. Seehra, V. S. Babu, A. Manivannan, and J. W. Lynn, Phys. Rev. B: Condens. Matter **61** (5), 3513 (2000).
7. M. S. Seehra and A. Punnoose, Phys. Rev. B: Condens. Matter **64** (13), 132410 (2001).
8. A. Punnoose, T. Phanthavady, M. S. Seehra, N. Shah, and G. P. Huffman, Phys. Rev. B: Condens. Matter **69** (8), 054425 (2004).
9. E. L. Duarte, R. Itri, E. Lima, Jr., M. S Baptista, T. S. Berqué, and G. F. Goya, Nanotechnology **17**, 5549 (2006).
10. T. S. Berqué, J. J. Erbs, A. Lindquist, R. L. Penn, and S. K. Banerjee, J. Phys.: Condens. Matter **21**, 176005 (2009).
11. N. J. O. Silva, V. S. Amaral, A. Urtizberea, R. Bustamante, A. Millán, F. Palacio, E. Kampert, U. Zeitler, S. de Brion, Ó. Iglesias, and A. Labarta, Phys. Rev. B: Condens. Matter **84** (10), 104427 (2011).
12. J. G. E. Harris, J. E. Grimaldi, D. D. Awschalom, A. Chiolero, and D. Loss, Phys. Rev. B: Condens. Matter **60** (5), 3453 (1999).
13. C. Gilles, P. Bonville, H. Rakoto, J. M. Broto, K. K. W. Wong, and S. Mann, J. Magn. Magn. Mater. **241**, 430 (2002).
14. N. J. O. Silva, V. S. Amaral, and L. D. Carlos, Phys. Rev. B: Condens. Matter **71** (18), 184408 (2005).
15. N. J. O. Silva, A. Millán, F. Palacio, E. Kampert, U. Zeitler, H. Rakoto, and V. S. Amaral, Phys. Rev. B: Condens. Matter **79** (10), 104405 (2009).
16. R. P. Guertin, N. Harrison, Z. X. Zhou, S. McCall, and F. Drymiotis. J. Magn. Magn. Mater. **308**, 97 (2007).
17. D. A. Balaev, A. A. Krasikov, A. A. Dubrovskiy, S. V. Semenov, S. I. Popkov, S. V. Stolyar, R. S. Iskhakov, V. P. Ladygina, and P. H. Yaroslavtsev, Phys. Solid State **58** (2), 287 (2016).
18. D. A. Balaev, A. A. Dubrovskii, A. A. Krasikov, S. V. Stolyar, R. S. Iskhakov, V. P. Ladygina, and E. D. Khilazheva, JETP Lett. **98** (3), 139 (2013).
19. D. A. Balaev, A. A. Krasikov, A. A. Dubrovskii, S. V. Semenov, O. A. Bayukov, S. V. Stolyar, R. S. Iskhakov, V. P. Ladygina, and L. A. Ishchenko, J. Exp. Theor. Phys. **119** (3), 479 (2014).
20. D. A. Balaev, A. A. Krasikov, A. A. Dubrovskii, O. A. Bayukov, S. V. Stolyar, R. S. Iskhakov, V. P. Ladygina, and P. H. Yaroslavtsev, Tech Phys. Lett. **41** (7), 705 (2015).
21. S. V. Stolyar, O. A. Bayukov, Yu. L. Gurevich, V. P. Ladygina, R. S. Iskhakov, and P. P. Pustoshilov, Inorg. Mater. **43** (6), 638 (2007).
22. S. V. Stolyar, O. A. Bayukov, Yu. L. Gurevich, E. A. Denisova, R. S. Iskhakov, V. P. Ladygina, A. P. Puzyr', P. P. Pustoshilov, and M. A. Bikhetina, Inorg. Mater. **42** (7), 763 (2006).

23. Yu. L. Raikher, V. I. Stepanov, S. V. Stolyar, V. P. Ladygina, D. A. Balaev, L. A. Ishchenko, and M. Balasoiu, Phys. Solid State **52** (2), 298 (2010).

24. A. D. Balaev, Yu. V. Boyarshinov, M. M. Karpenko, and B. P. Khrustalev, Prib. Tekh. Eksp., No. 3, 167 (1985).

25. M. Balasoiu, S. V. Stolyar, R. S. Iskhakov, L. A. Ischenko, Y. L. Raikher, A. I. Kuklin, O. L. Orelovich, Yu. S. Kovalev, and T. S. Kurkin, Rom. J. Phys. **55** (7–8), 782 (2010).

26. S. V. Stolyar, O. A. Bayukov, V. P. Ladygina, R. S. Iskhakov, L. A. Ishchenko, V. Yu. Yakovchuk, K. G. Dobretsov, A. I. Pozdnyakov, and O. E. Piksina, Phys. Solid State **53** (1), 100 (2011).

27. D. Tobia, E. Winkler, R. D. Zysler, M. Granada, H. E. Troiani, and D. Fiorani, J. Appl. Phys. **106**, 103920 (2009).

28. J. C. Denardin, A. L. Brandl, M. Knobel, P. Panissod, A. B. Pakhomov, H. Liu, and X. X. Zhang, Phys. Rev. B: Condens. Matter **65** (6), 064422 (2002).

29. E. C. Stoner and E. P. Wohlfarth, Philos. Trans. R. Soc. London, Ser. A **240**, 599 (1948).

30. S. V. Komogortsev, R. S. Iskhakov, A. D. Balaev, A. V. Okotrub, A. G. Kudashov, N. A. Momot, and S. I. Smirnov, Phys. Solid State **51** (11), 2286 (2009).

31. L. Néel, C. R. Hebd. Seances Acad. Sci. **252**, 4075 (1961).

32. J. T. Richardson, D. I. Yiagas, B. Turk, K. Forster, and M. V. Twigg, J. Appl. Phys. **70**, 6977 (1991).

Translated by O. Borovik-Romanova